RESEARCH OF PLASMA ACCELERATION PROCESSES IN SELF-FIELD AND APPLIED MAGNETIC FIELD THRUSTERS.

V. B. Tikhonov, S. A. Semenihin
Moscov Aviation Institute.

V. A. Alexandrov, G. A. Dyakonov, G. A. Popov
Research Institute of Applied Mechanics and Electrodynamics Moscov Aviation Institute.

Abstract.

In most of scientific vorks, dealing vith plasma acceleration processes in MPD thrusters, published in an earlier period (60-70-s) as vell as during the last 8-10 years, special attention vas payed to the problems of continuous and stable plasma flov acceleration from lov (subsonic)velocities to velocities significances higher than sound velocity.

Hovever, interconnection of flov parameters and magnetic field,defining plasma acceleration processes, is not clearly knovn. In particular the character of such interconnection defines conditions of plasma acceleration stability and plasma flov boundary formation, vhich may not correspond to electrode system geometry.

1. Introduction.

In the article by professor Jahn [1], vhere the main investigation problems for future EPT are stated, the necessity of ingeneering methods of plasma parameters, current and magnetic field distributions and thrusters characteristics calculation creation is marked. Special attention is payed to definition of stable thruster's vork, optimal electrode geometry and vays to decrease electrode temperature and erosion. The stated data of investigations results shoves that the use of lithium as a propellant allies to obtain higher levels of MPD thrusters efficiency [2] vith simultaniouse decrease of cathode erosion.

MPD thrusters tests on quasistationary modes allov to make a model of plasma flov dynamic processes vith high pover levels.

In differ to adopted in most of published theoretical investigations on plasma acceleration processes in MPD thrusters, in the present paper a concept of plasma flov vith movable boundaries and changing boundary conditions is adopted.

Published vorks presented on scientific conferences analysis shoves, that quasi-one-dimensional approximation describes peculiarities of plasma acceleration processes in MPD thrusters rather good to use it in the present paper.

2. Theoretical analysis of plasma acceleration processes in self-field MPD thrusters.

This type of thrusters coves Coaxial High Current Thrusters (CHCT) and Butt High Current Thrusters (BHCT). A scheme of BHCT is shovn on

fig.1. Possibility of implementation of variety of acceleration processes in such thrusters is described in [3].

The concept of plasma, flow boundary mobility can be used with a condition of electromagnetic forces prevalence on gas-dynamic forces, which means within such modes of MPD thrusters operation, when $P_m/P_{g.d.} \geq 1$. This relation can be presented in such a form,

$$\frac{P_m}{P_{g.d.}} = \frac{k\mu_0}{8\pi} \frac{I^2 M}{\dot{m} a} = A \qquad (1)$$

where $k = C_p/C_v$; I - current; $\dot{m}$- mass flow; M - mach number; a- sound velocity.

Relation $P_m/P_{g.d.}$ is a criterion of similarity of plasma flow.

With $A \ll 1$ gasdynamic acceleration prevails, which is characteristic to Arcjet Thrusters, and plasma flow boundary in formed by the channel walls (electrodes). With $A \geq 1$ volumetric electromagnetic forces prevail. They accelerate the flow and form its boundaries.

Naturally, the two extreme cases, $A \ll 1$ and $A \geq 1$ require different approaches, to construction forms of channel geometry and thrusters electrodes.

As the most efficient modes for MPD thrusters are the modes of electromagnetic acceleration, when $A \sim I^2/\dot{m} > 1$, we will analyze this case.

In any MPD thrusters type areas of gasdynamic (heating) subsonic flow acceleration and electromagnetic supersonic flow acceleration do exist.

In SHCT with propellant feed through multi hollow cathode the area of gasdynamic acceleration of subsonic flow is well determined. With $A \geq 1$ magnetic field holds plasma. On external flow boundary electrons are magnetized and charged particles diffusion across magnetic field is rather small. That is why one may consider that on the flow boundary $\vec{j} \| \vec{v}$. As this condition is satisfied on the axis, it is satisfied in all the volume. Then the work of volumetic forces $\vec{j} \times \vec{B} \vec{v} = 0$, and the only factor accelerating the flow is soul heating j^2/σ. While transition trough M=1 flow acceleration is more efficient by means of volumetric electromagnetic forces. Condition $\vec{j} \| \vec{v}$ becomes unsatisfied. Left boundary of this area near the cathode butt is rather stable, and the value of velocity and M number may be determined from the following.

$$\frac{P_{m\ bound}}{P_{g.d.\ aver}} = A = 1$$

From (1) one can determine M at the end of ionization area at the exit of cathode with accuracy of sound velocity.

$$M = 1.2\, a\, \dot{m}\, 10^7/I^2$$

As in MGD flows magnetic (fast) sound velocity $C_m = (C_A^2 + a^2)^{1/2}$, where C_A - Alfven velocity, is a characteristic velocity of disturbance spread, a problem of continuous transition through critical velocity C_m conditions arises. Interconnection between numbers $M = v/a$, $M_m = v/C_m$ and A number is defined by the

following relation:

$$M_m = M(1+1.2A)^{-0,5} \quad \text{with}$$

$$k = C_p / C_v = 5/3 \qquad (2)$$

It follows from (2) that in MPD thrusters with one stage with the increase of A, even with M=1, the flow remaines subcritical.

In two-stage schemes with supersonic flow from the first stage a limitation on $A \sim I^2/\dot{m}$ value exists. Besides that in such schemes limitation connected with possible transition trough drift velocity $v_{dr} = E/B$ is also present.

This two characteristic peculiarities may be demonstrated on the most simple example of coaxial thruster with constant cross section.

The system of equations for this thruster in nondimensional values is [9]:

$$\overrightarrow{\rho v} = 1 \qquad (3)$$

$$kM_o^2 d\bar{\vartheta} + d\bar{\rho} + A_o d(\bar{B}^2) = 0 \qquad (4)$$

$$\frac{k-1}{2} M_o^2 \, d(\bar{\vartheta}^2) + d\bar{T} + \frac{k-1}{k} \frac{2A_o}{\Pi_o} d(\bar{B}) = 0 \qquad (5)$$

$$\bar{p} = \bar{\rho}\bar{T} \qquad (6)$$

$$\bar{j}_r = \bar{\sigma}(1 - \Pi_o \bar{\Pi}) \qquad (7)$$

$$\bar{\sigma} = \bar{T}^{3/2} \qquad (8)$$

$$\bar{j}_z = - d\bar{B}/d\bar{z} \qquad (9)$$

where $\bar{\rho} = \rho/\rho_o$ and so on; $\Pi = vB/E$

In the system (3)-(9) there are three criteria, defining the character of plasma flow M, Π, A and only one equation (9), demanding numerical integration. In coordinate plan M-Π the boundaries of supersonic flow acceleration are well defined [9] $M \geq 1$, $k-1/k \leq \Pi \leq 1$.

This allowes to define the area of stable thrusters operation by means of solution of the system (3)-(9) with the following boundary conditions:

$z=0$ $\bar{B}=1$ $z=l$ $\bar{B}=0$ $z=0$ $M \geq 1$

$0 \leq \Pi \leq k-1/k$ $z \leq l$ $M>1$ $\Pi_{max} \leq 1$

The first condition B=0 with z=l consider total outflow of current inside the thruster. The second - the absence of flow stagnation to M<1 and impossibility of transition through drift velocity.

Boundaries of stable operation with $M_o = 2.29$ at the inlet of the channel are shown on Fig.2. With $M_o = 2.29$ it follows from (2) that three is a limitation on the value of A_o connected with smooth transition through magnetic sound velocity $A \leq 3.93$. Calculations shoves significant influence of A_o on the character of current outflow along the axis (Fig.3). With the increase of A_o the length of current outflow increase, however, when reach drift velocity inside the channel (large A_o) only small part of current outflows inside the channel (curve 3). The rest of current flows out of the electrode system.

This is one of the reasons for coaxial thruster degeneration to butt (end-fire) thruster.

Variation of $j_r(z)$ is shown on fig.4, where

experimental data, obtained in [4] are given. The character of calculation and experimental data values correspond.

The second reason is cooperative action of pinch and Hall effects, decreasing particles density near the anode, increasing longitudinal current density j_z and correspondingly current outflow out the electrode system.

Main peculiarities of **BHCT** are the following:

- location of ionization area inside multihollow cathode and near its surface while propellant feed trough the cathode:
- continuity of transition from subcritical to supercritical velocities ($M_m>1$ with any value $A_o \sim I^2/\dot{m}$;
- necessity to profilate anode geometry in correspondence with flow;
- possibility of existence of a number of acceleration processes.

For theoretical calculation of **MPD** thrusters parameters and characteristics the last three peculiarities are of greatest importance.

Possibility of different acceleration processes comes from Bernulli integral for magnetogasdynamic flows [9]

$$\frac{v^2}{2}+\int\frac{d\rho}{\rho}+(10^{-7}/\dot{m})\int v\,dI=\text{const} \qquad (10)$$

It follows from (10), that with different functions $p(\rho)$ and $v(I)$ different processes may exist.

As plasma temperature is approximately constant a set of isotermic process may be considered. One of the possible processes, connected with $v(I)$ and $M(I)$ functions type with $T=\text{const}$ is the process of acceleration with satisfaction of "freezing" condition $B/\rho r=\text{const}$.

It is easy to show, using mass flow equation $\dot{m}=\rho vS=\text{const}$, Amperes law $B=\mu_o I/a\pi r$ and condition $B/\rho r=\text{const}$ that function $v(I)$ is of the following form:
$vI=\text{const}$ or $MI=\text{const}$.

Such mode of flow is possible if magnetic Reynolds number is greater than 1 $Re_m=\mu\sigma vl \sim 10$.

Equation (10) in non-dimensional form is the following:

$$kM_o^2(\bar{M}^2-1)/2+\ln\bar{\rho}+2\alpha A_o\int\bar{M}\,Id\bar{I} \qquad (11)$$

where A_o - relation of magnetic pressure of flow boundary to average static pressure in it;

$\alpha=B^2_{aver}/B^2_{bound}$ averoging coefficient of magnetic pressure
$\alpha\sim0,5$ with $j_z(r)=\text{const}$

It follows from (11), that

$$p=\exp-[kM_o^2/2(\bar{M}^2-1)-2\alpha A_o(\bar{M}-1)/\bar{M}] \qquad (12)$$

Then, from mass flow continuity equation, flow cross section as function of M number is determined:

$$\bar{s}=1/\bar{p}\bar{M} \qquad (13)$$

This means, that every mode on current and massflow, its own flow geometry corresponds to, to which electrode geometry must correspond.

However, function $\bar{I}=\bar{M}^{-1}$ is a special form of the exponent function. In general it is worth to consider function $\bar{I}=\bar{M}^{-n}$, where $n>0$. Then, using the system of **MGD**

equations in quasionedimensional approximation, one may obtain the folloving relations for flov parameter and magnetic fields determination, taking into account EMF of Hall in the Ohm is lav with T=const:

$$p=\exp-[kM_o^2/2(\bar{M}^2-1)-2\alpha A_o/(1-2n)*(M^{1-2n}-1) \quad (14)$$

$$\bar{s}=1/p\bar{M};\ \bar{R}=\overline{s^{0.5}} \quad (15)$$

$$\bar{B}=1/s^{0.5}M^n \quad (16)$$

$$\bar{j}_z=\bar{\rho}\bar{M}^{1-n} \quad (17)$$

$$\bar{j}_r=Re_{m_o}(1-\Pi M_o^{1-n}- -\zeta_o\Pi_o M^{1-2n})/2\Pi_o\bar{R} \quad (18)$$

$$\bar{z}=\Pi_o/2Re_m\int_o(kM_o^2\bar{M}+(2n-1)\bar{M}^{-1}- -2\alpha A_o n\bar{M}^{-2})/(1-\Pi_o\bar{M}^{1-n}\zeta_o\Pi_o\bar{M}^{1-2n})/\bar{M}^n dM \quad (19)$$

Subscript "O"relates to flov cross section, vhere M =M_o. In one stage schemes Mo=1.
Correspondingly in this cross section value of A_o is equal to:

$$A_o=0.899*10^{-7}I^2/\dot{m}a \quad (20)$$

Parameter $\zeta_o=IM_i/e\dot{m}$- relation of current to mass flov in current units (M_i - ion mass, l - electrone charge).

With small values of Hall parameter and big Re_m EMF of Hall may be neglited, and then in equation (19) there is only one limitation, connected vith impossibility of transition through drift velocity at end of gasmagnetic acceleration area.

$j_r=-1/\mu_o dB/dz \le 0$ vith $M = M_o$

One may obtain from that vith M=1:

$$2\alpha A_o \le (kM_o^2+2n-1)/n \quad (21)$$

or, vith n=1 and α~0,5

$$A_o \le kM_o^2 + 1 \quad (22)$$

Hovever, one should take into account, that vhile flov acceleration to velocities close to drift velocity ($\Pi \le 1$; $j_r=-1/\mu_o dB/dz$~0) even a small value of Hall EMF may lead to magnetogasdynamic instability. This helps to form current vortexes near the anode surface, vhich becomes knovn vhile parameters calculation in tvo-dimensional approximation (fig.5).

If take into account Hall EMF, one should take into account one more limitation, vhich follov from (19):

$$\zeta_o \le (1-\Pi_o)/\Pi_o \quad (29)$$

9. Onset phenomenon in MPD thrusters and ion sound instability.

Onset phenomenon, limiting MPD thrusters characteristics, has been videly discussed in scientific literature, for example in [5]. First calculations, made by us, shoved, that vith the increase of $A_o \sim I^2/\dot{m}$ accelerating flov diameter decreases. That is vhy, it vas vorth to search for the boundary of stable modes in non-dimensional coordinates plane $A_o=f(D_a/D_c)$.

Generalization of experimental volt-Ampere

characteristics of MPD thrusters, operating in stationary and quasistationary modes with variouse propellants, alloved to determine boundary of stability [9], which is shovn on fig.6.

Knoving the boundary, one may determine critical currents with knovn D_a/D_c and $\dot{m}$:

$$I_{cr} = 1.2\ 10^{7} \dot{m} a A_{ocr} \qquad (24)$$

As physical peculiarities of charge transfere into anode are similar to that with presence of external magnetic field near the anode surface. Then for MPD thruster with applied magnetic field the boundary of stability does not change, if use instead of A_o similar by sense value:

$$A_o' = \frac{I B_c (R_a - R_c) 10^{-7}}{\mu_o a \dot{m}} \qquad (25)$$

vhere B_c - magnetic induction at the end of cathode;
R_a, R_c - anode and cathode radii

Therefore, ion sound instability boundary is universal for both MPD thrusters types and any propellants.

Experimental data on onset phenomenon, given in [6], are in good correspondence vith (24). In experiments vith thruster DT-5 in Stuttgart University vith relation

$D_a/D_c = 4.9$;

$A_{ocr} = 0.7$ (fig.6) for Argon (Ar) propellant and $T_e \sim 1eV$, it follovs from (24):

$$I_{cr}^2 = 2.4\ 10^{10} \dot{m}$$

As can be seen from fig.7, calculation and experimental values are practically the same.

4. Characteristics of self field MPD thruster.

Folloving relations are the basis for calculation:

- relation of thrust in respect of current $T(I^2)$;
- relation of voltage in respect of current $U(I)$.

Used for thrust calculation equations:

1. $T = 10^{-7} \ln(R_a/R_c)_{eff} I^2$ and

2. $T = (0.75 + \ln(R_a/R_c)) 10^{7} I^2$

are not acceptable for tvo reasons. With changeable electrode geometry, $(R_a/R_c)_{eff}$ can not be constant.

Basing on the concept of accelerating plasma flov boundary movability and relations, obtained above, relation for thirst vas obtained from impulse equation in the form [9]:

$$T = (0.5 + .899 M_o^2 A_o^{2(1-n)(2n-1)} + 0.5 A_o^{-2n(2n-1)}) 10^{7} I^2 \qquad (26)$$

With $n=1$ and $M_o = 1$(one stage scheme) relation (26) significantly reduces:

$$T = (1.99 + 0.5 A_o^{-2}) 10^{-7} I^2 \qquad (27)$$

Thrust coefficient $k_T = (1.99 + 0.5 A_o^{-2})$ depends on $I^2/\dot{m}$ and is a variable. With the increase of A_o flov boundary radius, decrease and relatively decrease the volume, vhere electromagnetic forces act. By this the fact of decrease of K_T with increase $I^2/\dot{m} \sim A_o$ is explained.

and not by friction in boundary layer, as stated in [7]. Experimental data, given in this article, dealing with K_T variation approve not only quantitative but qualitative correspondence of obtained relation (Fig.8). Relations (26) and (27) are acceptable with $A_o \geq 1$. With $A_o < 1$ gasdynamic component of thrust plays its role.

Theoretical determination of thruster's Volt-Ampere characteristic by means of integral $U=\int Edl$ is rather difficult. Much easier to determine Volt-Ampere characteristic (VAC) through energy expenditures on thruster's processes [9].

Volt-Ampere characteristic for lithium thruster with pover up to 500 kW is given on fig.9.

The influence of electrode geometry on BNCT efficiency is shovn on fig.10.

For example of correspondence calculation and experimental data, experimental characteristics of MPD thruster obtain in [8] are given on fig. 11 and 12 together with calculated according to above relations curves.

Fig. 13 and 14 shov nomograms of BHCT characteristics for H_2 and Li.

It is easy to shov, that with A_o=const specific impulse I_{sp}=const. Using relation for thrust (27) and (20) one may obtain:

$$I_{sp} = 1.2\, a_o A_o (1.33+0.5A_o^{-2}) \quad (28)$$

It was shovn above, that the value of A_o has a limitation, that is vhy specific impulse of one stage MPD thruster is limited. As can be seen from characteristics on fig. 13 and 14, from the point of viev of high efficiency with acceptable specific impulse and lov voltages, advantages of lithium are of no doubt.

Plasma flov parameters calculation in two-dimensional MGD approximation on the model of slovly changing channel approved the fact, that A_o is a criterion of similarity of plasma flov.

Plasma flov parameters distribution along the length, shovn on fig..15 are identical vith preservation of condition $A_o \sim I^2/\dot{m}$= const.

5. MPD thrusters vith Applied Magnetic Field (Butt(End-fire) Hall thrusters BHT).

The scheme of BHT differs from that of BHCT only by presence of coil, producing external magnetic field. Only experimental investigation of distributions of currents, magnetic fields and plasma parameters inside the thruster and in the outflov alloved to receive physical model of acceleration process and to develope methods of calculation of BHT characteristics. This measurements probe vith the help of three component magnetic probe vith Hall-type sensors vith lithium propellant vith pover up to 40kW [9].

There are two characteristic areas of flov acceleration. First has the outer boundary, defined by magnetic force line, passing through outer cathode diameter. It is the area of previaled gasdynamic accelearation ($\bar{j} \,||\, \bar{B}_{out}$). The second area of electromagnetic acceleration is

located from the boundary of the first area to magnetic force line, passing through the exit anode edge. In this area $J_z \sim 0$. Radial component of current dencity j_z is practically constant along the length. On the upper boundary of this area electrones are moving along magnetic force line of external magnetic field.

Repeat experiments on the BHT model shown on fig. 16 not only approved results obtained earlier, but gave a number of new. Firstly, profilating of anode along magnetic field resulted in uniform distribution of energy, brought by electrones to the anode. In comparision with cylindrical anode temperature decreased by more than 1.5 times and was ~ 2000K.

Results of magnetic probes measurements are given on fig. 17, 18 and 19.

Secondly, electrone temperature and plasma dencity measurements by electric probes showed, that T_e increased with the increase of radii and reached 4-5 eV near the anode surface. Particles dencity was greater on the axis and decreased towards the anode. Ion velocity vector, determined by rotating electric probe by maximal ion current, at thruster's exit was all most the same as magnetic force line direction. All this served as a basis for obtaining calculational relation for BHT thrust in respect of current and magnetic field.

Hall component of electromagnetic thrust $T_h = \int j_u B_r dv$ can be defined in the folloving form:

$$T_H = I/\pi l_{ca} S_a B_a (1 - B_a/B_c)[1 + 0.5 * \ln(B_c/B_a) - S_c B_c/S_a/B_a + 0.5 S_c B_c/S_a/B_a] \quad (28)$$

where $B_c S_c$, $B_a S_a$ magnetic field and cross section near cathode and anode.

Magnetic probing showed, that Hall currents j_θ and accelerating volumetric force $j_\theta B_r$ are located inside the thruster with distance between cathode and anode edge $l_{ca} \sim D_a$. Then (28) can be represented in the folloving form:

$$T_H = K_T I B_a D_a \quad (30)$$

This relation corresponds to physical sense and thrust coefficient can alvays be determined with given electrodes dimensions and magnetic field.

Electromagnetic component of thrust from discharge current can be defined as magnetic pressure on cathode edge.

$$T_I = K_T 10^{-7} I^2$$

Gasdynamic component produced by impulse change while propellant flov out of cathode

$$T_{gd} = 1.4 \dot{m} \sqrt{kT_e/M_i}$$

Total BHT thrust will be:

$$T = K_T I B_a D_a + K_T * 10^{-7} I^2 + 1.4 * \dot{m} (kT_e/M_i)^{0.5} \quad (31)$$

Volt-Ampere characteristic calculation can be made according to methode of energy expenditures balance.

Results of experimental determination of characteristics of the model with profilated anode and multi hollov cathode (fig. 16)

are shown on fig. 20, 21, 22.

To determine electrode system dimensions of the thruster, currents and magnetic fields a set of characteristics, given on fig. 23, may be defined. From (25) the critical value of magnetic induction can be determined with given electrodes dimensions for any current and mass flow.

6. Investigation of MPD thrusters in quasistationary modes.

Accelerator, developed in RIAME MAI (fig.24) consists of pulsed electromagnetic value for gas feeding and electrodes. In the process of investigations experimental verification of the influence of cathode and anode as well as external magnetic field on thrusters volt - Amperes characteristics as currents outflow was made. The following variants of electrode system were investigated (fig. 25). In the electrical scheme timing of mass input into accelerator channel and discharge current was made. Fig. 26 shows oscillogramm of current and voltage. Oscillations on the curve of voltage are observed when critical current modes are reached.

Electrode geometry influence on volt-Ampere characteristic is well seen on fig. 27. On fig. 28 Volt-Ampere characteristic, showing the influence of longitudinal field on discharge voltage, is shown.

Characteristic feature is, that with mass flow $\dot{m}$=0.55g/sec discharge voltage U~200V. This is rather close to the value, corresponding to MPD thruster characteristics nomogramm with hydrogen with current 15kA(fig. 14).

Character of variation of relative outflow currents value $\overline{I}/I_d$ in connection with discharge current and mass flow without external magnetic field and with it is shown on fig. 29 [10]. With the existence of magnetic field outflow currents increase efficiently with A>1 and stop at the level approximately 40% of discharge current. The increase of current outflow begins from the mode, when magnetic fields begin to form flow boundary. Magnetic probing of outflow currents in stationary give the same value.

Conclusion.

Theoretical analysis of processes of acceleration in quasi one dimensional approximation taking into account plasma flow boundary mobility and obtained on its basis thrusters characteristics showed good correspondence with experimental data.

MPD thrusters characteristics improvement as well as its specific parameters demands coordination of electrode system geometry, geometry and value of external magnetic field with accelerating plasma flow geometry.

Main limitation on obtaining high specific impulse and efficiency is ion sound instability. Experimentally determined boundaries of stability allows to determine necessary dimensions of electrodes, currents, mass flows and magnetic fields on the stage of design which ensure necessary parameters.

Comparative analysis of thrusters characteristics

working on lithium and hydrogen shows that the use of lithium is promising from the point of view of high efficiency, as well as compatibility of characteristics of nuclear power station with thermoemittive energy transformer of "Topaz" type and lithium MPD thrusters self-field and with applied magnetic field. Within range of power 90=100 kW the most promising are lithium BHT. The problem of lithium condensation on vehicles surfaces while using nuclear power station demand separate dissension.

References

1. RG Jahn "Basic Research for Future Electric Propulsion". AIAA-85-965, 1985, Alexandria, Virginia.

2. J.E. Polk, T.J. Pivirotto. "Alkali Metal Propellants for MPD Thrusters". AIAA 91-3572 p. 1-21. 1991, Cleveland, OH.

3. N.V. Belan, V. Kim, A.I. Oranstky, V.B. Tikhonov. Stationary Plasma Thrusters. KhAI, Kharkov, 1989, pp. 985. in Russian.

4. M. Wolff, A.J. Kelly, R.G. Jahn, "A High Performance Magnetoplasmadynamic Thruster". IEPS-84-92 p. 206-212. Tokyo, 1984.

5. W.D. Merke, M. Auveter-Kurtz, H. Habiger, H. Kurtz, H.O. Schrade. Nozzle Type MPD Thruster Experimental Investigations. IEPS-86-028, p. 1-11, Carvisch-Patenkirchen, 1988.

6. H.O. Schrade, T. Wegmann, T. Rossgen "The Onset Phenomena Explained by Run-Away Joule Heating". IEPC-91-022, Viareggio, 1991.

7. J.H. Gilland, A.J. Kelly, R.G. Hahn. "MPD Thruster Scaling". AIAA-87-0997, p. 1-9, Colorado Springs, 1987.

8. H. Tahara, F. Takiguchi, Y. Kagaya, T. Yoshikava. Performance Characteristics and Discharge Features of a Quasi-Steady Applied-Field MPD Arcjet. IEPS-91-073, p. 1-11, Viareggio, 1991.

9. A.G. Popov, G. Ja. Portnov, S.A. Semenichin, V.V. Spiridonov, V.B. Tikhonov, V.H. Tikhonov. "Experimental investigation of magnetic fields and currents in Butt Hall Thrusters", Collection of papers "Ion injectors and Plasma accelerators", Moscov, Energoatomizdat, 1990, p. 97-105.

10. G.A. Dyakonov, V.B. Tikhonov. "Experimental research of outflow currents of papers to 7-th All-union conference on plasma accelerators and ion injectors", Harkov, 1989, p. 49-50. in Russian.

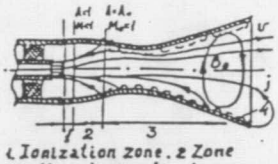

1. Ionization zone. 2 Zone gasdinamic acceleration.
3. Zone electromagnetical accel.
4. Anode Layer.

Fig.1. Butt High Current Thruster design.

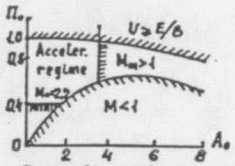

Fig.2 Stability boundaries for MHD flow in a channel of constant cross section

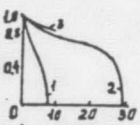

Axial distance sm

Fig.3 Current change in a channel

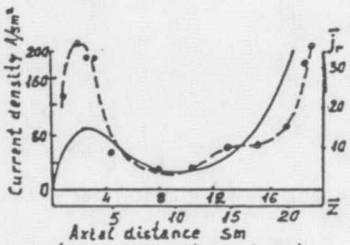

Axial distance sm

Fig.4. Current density distribution

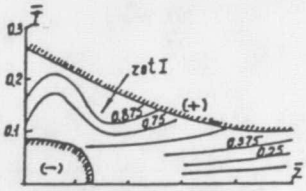

Fig.5 Current distribution.

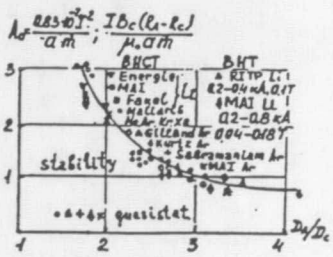

Fig.6 Boundary of ion-sound instability

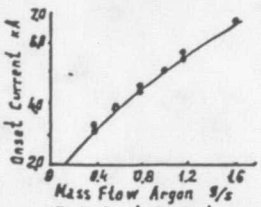

Mass Flow Argon g/s

Fig.7 Onset Current

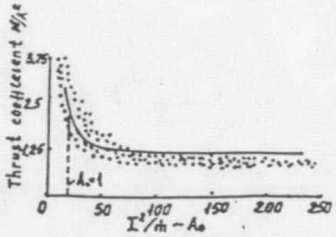

Fig.8 Thrust coefficient scaling

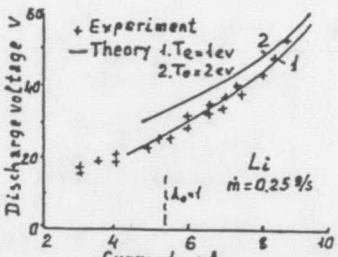

Fig.9 Volt-Current characteristic BHCT

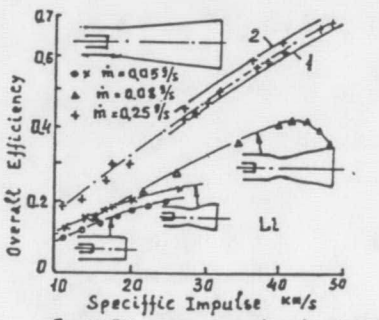

Specific Impulse km/s

Fig.10 Efficiency characteristics BHCT

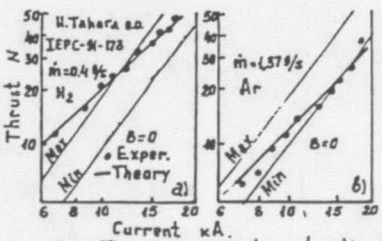

Current kA.

Fig 11 Thrust v.s. current caracteristics [8].

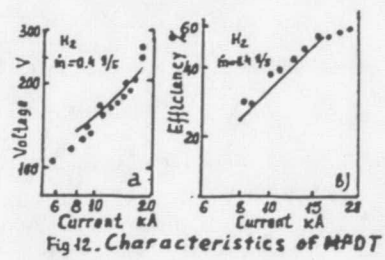

Fig 12. Characteristics of MPDT [8].

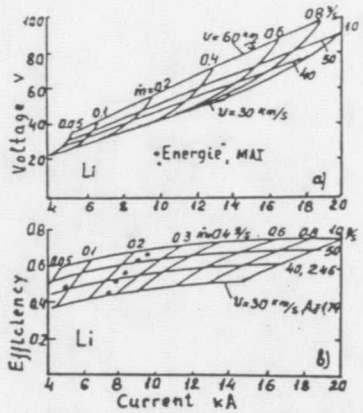

Fig.13 Nomogram of caracteristics BHCT

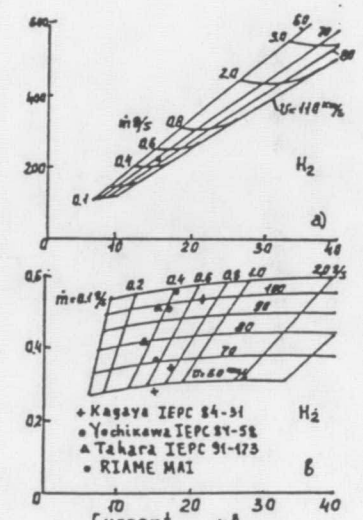

Fig.14 Nomogram of caracteristics BHCT. Prop. H_2

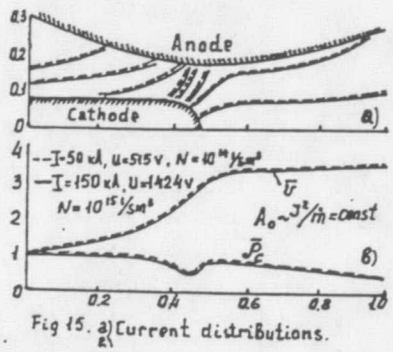

Fig 15. a) Current distributions.

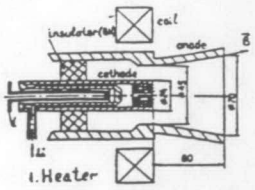

Fig.16. Butt Hall Thruster Design

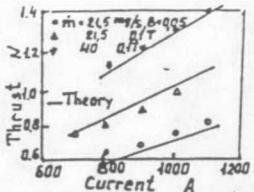

Fig.20 Thrust caracteristics BHT

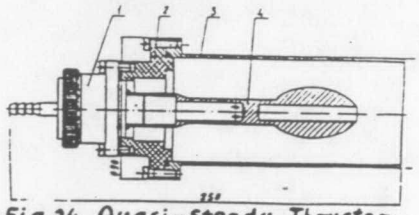

Fig.24. Quasi-Steady Thruster Design.

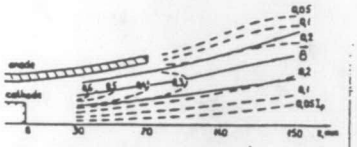

Fig.17 Current Distribution BHT

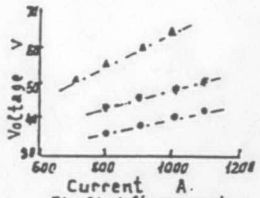

Fig.21 Volt-current caracteristics BHT

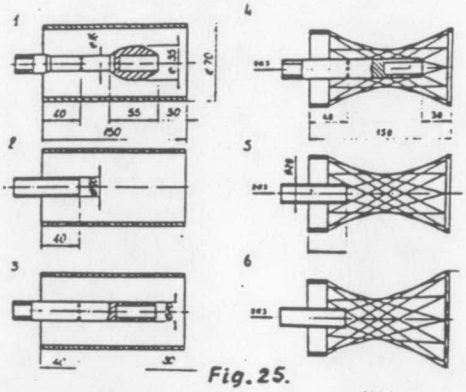

Fig.25.

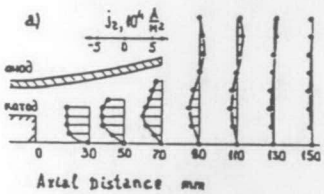

Fig.18 Current Density Distribution a. Radial, b. Azimuth

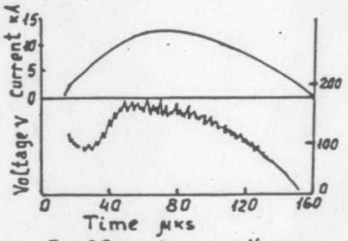

Fig.26 Discharge oscillogram

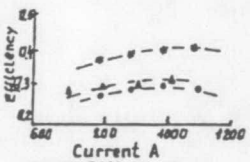

Fig.22 Efficiency caracteristics BHT

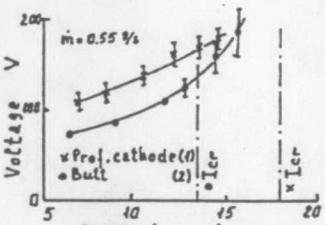

Fig.27 Volt-Curret caracteristics Quasi-Steadi Thrusters. H_2

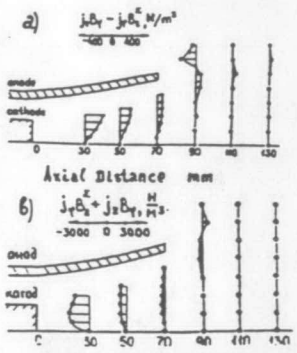

Fig.19 Force Distribution a) Axial force; b) Radial Force

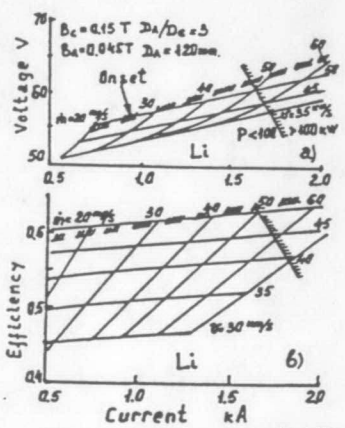

Fig.23 Nomogram caracteristics B.H.T: a) Volt-current; b) Efficiency

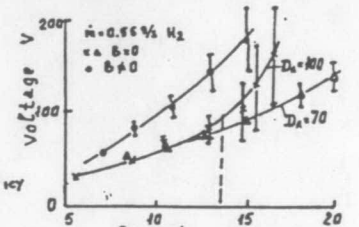

Fig.28 Comparison V-I Characteristics

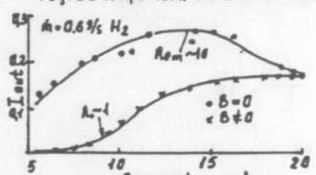

Fig.29 Current out v.s Current Characteristics.